

Infrared studies of the energy gap and electron-phonon interaction in potassium-tetracyanoquinodimethane (K-TCNQ)

D. B. Tanner

Department of Physics, The Ohio State University, Columbus, Ohio 43210

C. S. Jacobsen,* A. A. Bright,[†] and A. J. Heeger[‡]

Department of Physics and Laboratory for Research on the Structure of Matter, University of Pennsylvania, Philadelphia, Pennsylvania 19174

(Received 28 June 1976)

The polarized reflectance at room temperature of potassium-tetracyanoquinodimethane (K-TCNQ) has been measured. Analysis using the Kramers-Kronig transforms gives the response functions (dielectric function and conductivity) between 300 and 23 000 cm^{-1} . Attempts have been made to fit these functions with Lorentzian oscillators and it has been found that at least two such oscillators were required to give a satisfactory fit to the electronic transitions above 4000 cm^{-1} : a strong, sharp peak corresponding to interband transitions and a weaker, broader absorption at higher energy from an intramolecular excitation. The oscillator-strength sum rule indicates that the energy gap is much larger than that inferred from magnetic resonance measurements and supports the view that Coulomb correlations are important in K-TCNQ. The molecular stretching modes are found to be stronger for the infrared electric field along the chain axis than perpendicular to it. As shown by recent calculations, this effect arises from electron-optical-phonon coupling effects. From the infrared data, we estimate the dimensionless electron-optical-phonon coupling constant to be $\lambda_{\text{opt}} \sim 0.1$.

I. INTRODUCTION

In this paper we report the results of polarized reflectance studies in the infrared and visible (300–23 000 cm^{-1}) of K-TCNQ (potassium tetracyanoquinodimethane) and discuss these results in the light of several recent papers. We will show that in K-TCNQ there is evidence for *two* superimposed electronic transitions polarized along the chain axis for photon energies in the range 0.7–1.5 eV. In this we differ from the findings of Torrance, Scott, and Kaufman¹ in a recent study of optical properties of TCNQ salts. From the oscillator strength along the chain axis we will show that 90% of the direct electronic transitions occur for photon energies above 0.8 eV. This reinforces the conclusion of Khanna, Bright, Garito, and Heeger² that the optical energy gap in K-TCNQ is much larger than the triplet exciton excitation energy and hence that the Coulomb interaction in K-TCNQ is relatively strong, in contradiction to the analysis of Vegter and Kommandeur³ and Hibma and Kommandeur.⁴ Finally, we will discuss the molecular stretching modes of the TCNQ ion and the strength of their coupling to the electron gas. The data are analyzed in terms of recent calculations by Rice.⁵

Infrared and optical studies of K-TCNQ have been reported previously by a number of authors. Hiroma, Kuroda, and Akamatu⁶ have measured the polarized transmission between 8000 and 37 000 cm^{-1} , Khanna *et al.*² measured the polarized reflectance between 5000 and 27 000 cm^{-1} , and Ander-

son and Devlin⁷ measured the polarized reflectance between 600 and 3000 cm^{-1} of K-TCNQ crystals. All other experiments have been performed unpolarized on powder samples. These include the studies of Iida⁸ (4000–32 000 cm^{-1}), Vegter and Kommandeur³ (4000–44 000 cm^{-1}), Oohashi and Sakata⁹ (4000–36 000 cm^{-1}), Torrance, Scott and Kaufman¹ (4000–36 000 cm^{-1}), and Iqbal, Christoe, and Dawson¹⁰ (30–3500 cm^{-1}). The latter experiments are noteworthy for the temperature-dependent studies of the C \equiv N stretching modes. They found one of the three absorption lines in the vicinity of 2200 cm^{-1} weakened as the temperature was increased above 300 K, disappearing near 380 K. This is close to the temperature (400 K), where magnetic resonance measurements¹¹ indicate a phase transition.

II. EXPERIMENTAL TECHNIQUES

K-TCNQ crystals were grown by diffusion in an acetonitrile-filled U tube starting with KI and high-purity TCNQ. Crystals grown by this technique have been reported by Hoekstra, Spoelda, and Vos¹² to be quadruplets. The structure has been discussed very clearly by Hibma and Kommandeur.⁴ It is similar to that of Rb-TCNQ.^{4,12} Each crystal domain contains two types of stacks with the long axis of the molecule in two essentially perpendicular directions. In a given crystal the domains are arranged with all of their chain axes (the crystallographic \vec{a} direction) in the long (needle) direction while the crystallographic \vec{b}

direction of a domain is nearly parallel with the crystallographic \vec{c} direction of its neighbors. The optical properties parallel to the chain ($\vec{E} \parallel \vec{a}$) and perpendicular to it ($\vec{E} \parallel \vec{b}, \vec{c}$) are presumably independent of the domain formation. An important feature of the structure of K-TCNQ for the discussion in Sec. IV of this paper is the angle between the long axis of the TCNQ molecules and the chain axis. In Rb-TCNQ, the angle is¹² 76°; because of the similarity in the two salts, the angle in K-TCNQ is probably not very different. The chains in K-TCNQ are dimerized and the charge transfer is very nearly unity.

Polarized reflectance spectra were measured from 300 to 23 000 cm^{-1} with the specimen at room temperature. Over the frequency range 300–5000 cm^{-1} we used a Perkin-Elmer 225 spectrophotometer with wire grid polarizer and specular reflection insert, while between 5000 and 23 000 cm^{-1} we used a Beckman DK-2 spectrophotometer with a plastic polarizer and a homemade specular reflection insert described earlier.² In addition, the transmission of K-TCNQ powders were measured between 20 and 300 cm^{-1} as nujol mulls by Fourier-transform techniques and between 300 and 4000 cm^{-1} as KBr pellets with the PE 225. The results of these latter measurements were substantially the same as those of Iqbal, Christoe, and Dawson.¹⁰

III. EXPERIMENTAL RESULTS

Figure 1 shows the measured reflectance over the entire frequency range from 300 to 23 000 cm^{-1} . The data are shown for $\vec{E} \parallel \vec{a}$ as dotted lines and for $\vec{E} \parallel \vec{b}, \vec{c}$ as dash-dotted lines. The data show struc-

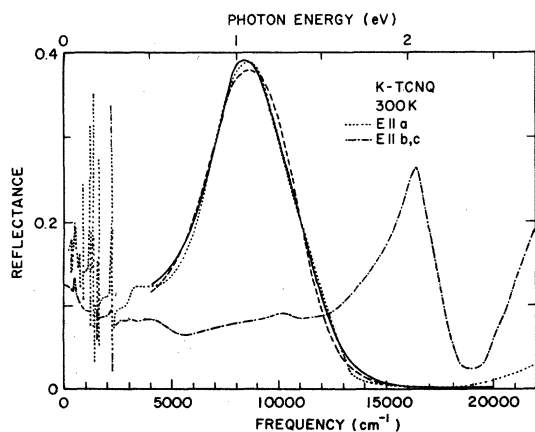


FIG. 1. Reflectance of K-TCNQ between 300 and 23 000 cm^{-1} . Data are shown for two polarizations. The dashed line is a fit of the reflectance for the electric field parallel to the chain axis by a single Lorentzian oscillator; the solid line is a fit to the two-oscillator model [Eq. (1)].

ture associated with molecular stretching and bending modes at low frequencies and a broad "metallic reflection" peak from direct electronic transitions at higher frequencies. Because of the wide bandwidth of the data, a Kramers-Kronig integral¹³ should give detailed information about line shapes and oscillator strengths in the molecular and electronic resonances. The following extrapolation schemes were employed to roughly simulate transitions above 23 000 cm^{-1} . R_{\perp} was continued smoothly to the value $R_0 = 0.28$ at $\omega_0 = 27\,000 \text{ cm}^{-1}$ and set equal to $R_0(\omega_0/\omega)^4$ for $\omega > \omega_0$. R_{\parallel} was smoothly joined to a $R_0(\omega_0/\omega)^2$ extrapolation with $R_0 = 0.04$ and $\omega_0 = 25\,000 \text{ cm}^{-1}$. These somewhat arbitrarily chosen extrapolations are expected to influence the level of the resulting $\sigma_1(\omega)$ and $\epsilon_1(\omega)$ data near the upper-frequency limits but not the line-shapes. In the frequency interval $0 < \omega < 300 \text{ cm}^{-1}$, R_{\perp} and R_{\parallel} were continued at their 300- cm^{-1} values as appropriate for a semiconductor.

IV. ELECTRONIC ABSORPTION

Recently, Torrance, Scott, and Kaufman¹ have proposed a universal explanation for the infrared and optical properties and for the dc conductivity of various TCNQ salts. It is based upon the observation of two absorption peaks polarized along the chain direction in the complex TCNQ salts (i.e., those with formally a fractional electron per TCNQ ion) and in the conducting salts. On the other hand, they apparently find only a single absorption peak polarized along the chain axis in K-TCNQ. They attribute the lower-energy peak to excitation of an electron from a TCNQ ion to a neighboring neutral TCNQ molecule and the higher-energy peak to excitations to a neighboring already occupied TCNQ⁻ ion. They describe the higher-energy peak as an interband transition and the lower-energy peak as an intraband transition (even though the complex salts are not conducting). Since K-TCNQ is fully charge transferred,¹⁴ the lower-energy peak would obviously not be seen. They conclude from the optical data that the conducting salts have less than integer charge transfer. X-ray^{15,16} and neutron-scattering¹⁷ measurements show that TTF-TCNQ has about 0.6 electron per TCNQ site. It has been suggested from magnetic measurements¹⁸ that NMP-TCNQ has about 0.96 electron per TCNQ site.

This interpretation, however, depends on there being only a single electronic absorption in K-TCNQ, polarized along the chain axis in the frequency region 4000–20 000 cm^{-1} . We will show that there is evidence that two such peaks are present. In Fig. 2, there is a peak in $\sigma_1(\omega)$ for $\vec{E} \parallel \vec{b}, \vec{c}$ clearly visible at 10 000 cm^{-1} . For $\vec{E} \parallel \vec{a}$ there is a strong transition at 7500 cm^{-1} . Khanna *et al.*² made a

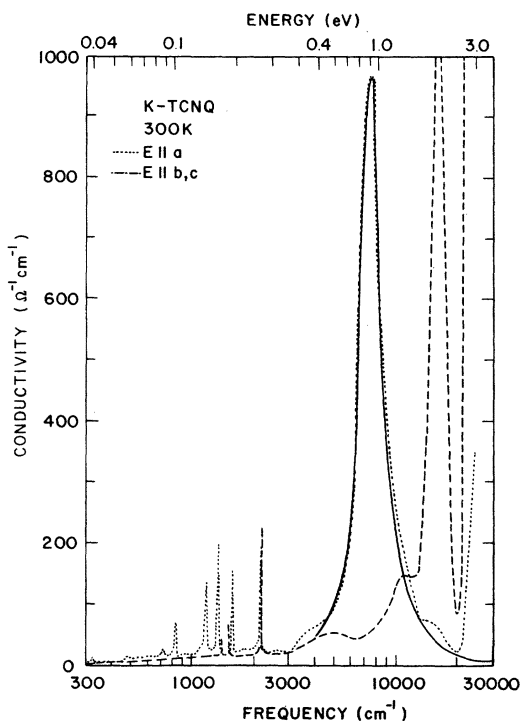


FIG. 2. Real part of the conductivity $\sigma_1(\omega)$ of K-TCNQ between 300 and 23 000 cm^{-1} . Note the logarithmic frequency since data are shown for two polarizations. The solid line is a fit of $\sigma_1(\omega)$ for the electric field parallel to the chain axis by two Lorentzian oscillators.

least-squares fit to the reflectance for $\vec{E} \parallel \vec{a}$ using a single Lorentzian dielectric function (as would be appropriate for a single absorption):

$$\epsilon(\omega) = \epsilon_{\infty} + \frac{\omega_p^2}{\omega_{sp}^2 - \omega^2 - i\omega/\tau}$$

The parameters used were $\epsilon_{\infty} = 1.28$, $\omega_p = 10\,100 \text{ cm}^{-1}$, $\omega_0 = 7120 \text{ cm}^{-1}$, and $1/\tau = 2300 \text{ cm}^{-1}$. The reflectance calculated from this dielectric function is shown as the dashed line in Fig. 1. The calculated reflectance fails to reproduce the structure on the high-frequency side of the reflectance maximum, falling below the measurement near the maximum crossing above at about 9000 cm^{-1} , and falling below it again between $11\,500$ and $13\,000 \text{ cm}^{-1}$.

The situation is substantially improved if a two-oscillator dielectric function is employed. This is given by

$$\epsilon(\omega) = \epsilon_{\text{core}} + \frac{\omega_L^2}{\omega_0^2 - \omega^2 - i\omega\Gamma} + \frac{\omega_p^2}{\omega_{sp}^2 - \omega^2 - i\omega/\tau}, \quad (1)$$

with the following values and definitions: $\epsilon_{\text{core}} = 1.50$ is the high-frequency dielectric constant; $\omega_L = 5000 \text{ cm}^{-1}$ is the strength, $\omega_0 = 10\,000 \text{ cm}^{-1}$ the center frequency, and $\Gamma = 6000 \text{ cm}^{-1}$ the width of a

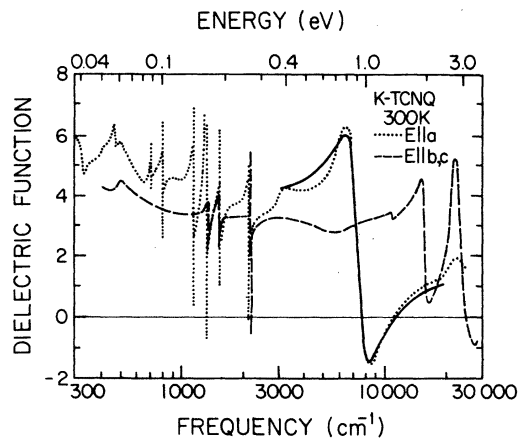


FIG. 3. Real part of the dielectric function $\epsilon_1(\omega)$ of K-TCNQ between 300 and 23 000 cm^{-1} . Note the logarithmic frequency scale. Data are shown for two polarizations. The solid line is a fit of $\epsilon_1(\omega)$ for the electric field parallel to the chain axis by two Lorentzian oscillators.

broad mode which is also present in the other polarization; $\omega_p = 10\,300 \text{ cm}^{-1}$ is the strength, $\omega_{sp} = 7470 \text{ cm}^{-1}$ the center frequency, and $1/\tau = 1980 \text{ cm}^{-1}$ the width of a strong sharp peak which is absent in the perpendicular direction. Using the two-oscillator dielectric function improves the reduced chi square of the fit by a factor of 3 (see solid line on Fig. 1). The upper-frequency peak is probably a low-lying excitation of the TCNQ $^{\cdot-}$, polarized in the plane of the ion, while the lower one is an interband transition across the semiconducting gap.

The real part of the conductivity and dielectric function calculated from Eq. (1) are shown as the solid lines in Figs. 2 and 3. Figure 4 shows, in a linear frequency plot, the measured conductivity for $\vec{E} \parallel \vec{a}$ (the points) and the calculation (shown as a solid line). The conductivities of the two individual oscillators which are summed to give the total conductivity are shown as the dashed and dot-dashed curves. If the strength of the dashed curve is increased by about 6%, it will fit reasonably well near the peak, but will fall far below the measurement above 9000 cm^{-1} .

While there is no *a priori* reason to suppose that a Lorentzian dielectric function describes the single-particle excitations in K-TCNQ, such a dielectric function gives a good description of other quasi-one-dimensional systems, such as TTF-TCNQ 19 and the platinum chain salts (KCP). 20 In the case of K-TCNQ the band gap is probably large compared to the bandwidths. If the bandwidths are small compared to the relaxation rates, then the Lorentzian oscillator (which describes a two-level system with lifetime effects broadening the transitions) will be an appropriate dielectric function.

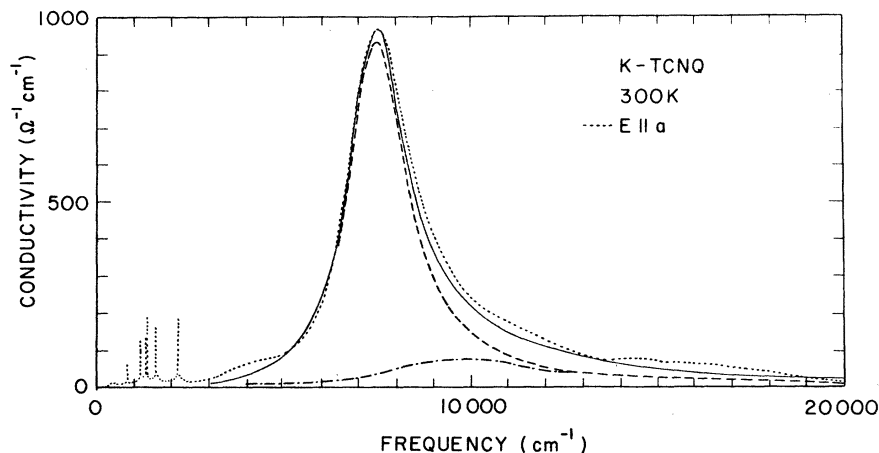


FIG. 4. Real part of the conductivity $\sigma_1(\omega)$ of K-TCNQ between 300 and 20 000 cm^{-1} for the electric field along the conductivity axis. The solid line is a fit to the data by two Lorentzian oscillators. The dashed lines show the two oscillators which are summed to give the solid line.

The failure of the single oscillator to fit the data implies that there are two nearly superimposed absorptions.

There seem to be two absorption peaks visible in the data for K-TCNQ of Torrance, Scott, and Kaufman.¹ In their absorption data, the stronger peak is centered at about 9000 cm^{-1} with very weak structure at 12 000 cm^{-1} . The powder absorption spectrum of Vegter and Kommandeur³ shows three peaks very clearly: a strong one at 8300 cm^{-1} and two weaker ones at 10 400 and 11 800 cm^{-1} . The polarized absorption spectrum of Hiroma, Kuroda, and Akamatu⁶ shows peaks at 7800 and 12 500 cm^{-1} , both polarized along the chain axis.

We conclude that there is evidence for at least two infrared electronic absorptions in K-TCNQ for polarization along the chain, just as there are in TTF-TCNQ and all of the other conducting and complex salts. The lower-energy one (at 1000 cm^{-1} in TTF-TCNQ¹⁹ and 7500 cm^{-1} in K-TCNQ) is an interband transition corresponding (in very general terms) to excitations of electrons along the chain. Above this, at 10 000–12 000 cm^{-1} (in both salts) is the lowest lying intramolecular excitation of the TCNQ⁻ ion. This interpretation is supported by measurements of the reflectance of TTF-TCNQ as a function of angle by Grant *et al.*²¹ which imply that the 10 000–12 000- cm^{-1} absorption has polarization components parallel to the long axis of the molecule and not only along the chain axis. Inelastic-electron-energy-loss measurements in TTF-TCNQ by Ritsko *et al.*²² show that the band is dispersionless throughout the Brillouin zone, characteristic of highly localized intramolecular excitation.

V. OSCILLATOR STRENGTH

Considerable information about the excitation spectrum of K-TCNQ can be extracted from the

oscillator strength sum rule. The effective number of electrons participating in optical transitions for energies less than $\hbar\omega$ is given by

$$\frac{m}{m^*} N_{\text{eff}} = \frac{1}{8} \int_0^\omega \sigma_1(\omega^1) d\omega^1 / \frac{4\pi N_c e^2}{m}, \quad (2)$$

where m^* is the band mass of the electrons and N_c is the number of molecules/unit volume. $N_c = 3.56 \times 10^{21} \text{ cm}^{-3}$ for K-TCNQ.¹² The result of this calculation is shown in Fig. 5. This shows $(m/m^*)N_{\text{eff}}$ for both polarizations and also for $\vec{E} \parallel \vec{a}$ magnified by a factor of 10. For the chain direction, $(m/m^*)N_{\text{eff}}$ is small until $\omega \sim 5000$ –6000 cm^{-1} ($\hbar\omega \sim 0.6$ –0.7 eV), where it rises very rapidly to a value of 0.43. As seen above, 70% of this oscillator strength comes from the interband transitions and the remainder from an intramolecular transition. At higher frequencies, the oscilla-

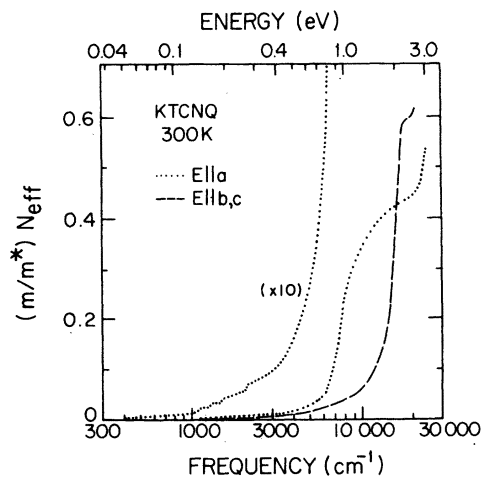


FIG. 5. The oscillator strength of K-TCNQ between 300 and 23 000 cm^{-1} . Notice the logarithmic frequency scale. Data are shown for two polarizations and for the electric field parallel to the chain axis magnified by 10.

tor strength rises again due to the onset of other intramolecular electronic excitations.

The principal point of Khanna *et al.*² was that the gap in K-TCNQ indicated by optical and transport measurements is larger than that inferred from magnetic resonance measurements. We wish to strongly reinforce that point here. The optical gap, as determined above, is $\hbar\omega_{sp} = 0.95$ eV. The temperature dependence of the dc conductivity indicates an energy gap (twice the activation energy) of approximately 0.7 eV. The relatively small difference between these two values may be due to uncertainty in the definition of the optical gap [thermally smeared onset of $\sigma_1(\omega)$ or peak in Lorentzian fit]. Alternatively, the difference may be genuine and be due to the minimum band gap being indirect (i.e., not a $\Delta k = 0$ electronic transition). In any case, the single-particle energy gap is much larger than the energy of the triplet exciton lines as determined by Hibma and Kommandeur⁴ as 0.24 eV (2000 cm^{-1}). These authors view the alkali-metal-TCNQ salts as simple semiconductors with this activation energy being the semiconducting band gap. However, as seen in Fig. 3, at this frequency ($m/m^*N_{eff} \sim 0.004$). Only 1% of the interband oscillator strength has been used up by this point. We conclude that this activation energy is *not* associated with the semiconducting (electronic) energy gap in K-TCNQ. The large value of the energy gap implies that the electron-electron Coulomb repulsive interaction U_{eff} is of the order of 0.9 eV ($U_{eff} \sim \hbar\omega_{sp}$), larger than the expected bandwidth. K-TCNQ, then, falls into the intermediate-to-strong Coulomb coupling regime in agreement with the conclusion of Khanna *et al.*² The activation energy measured by magnetic resonance techniques corresponds to spin wave or triplet excitons located within the single-particle gap. These excitations should be magnetic dipole active and would have transition probability weaker than the electric dipole active interband transitions by a factor of the fine structure constant squared ($\alpha^2 \approx 5 \times 10^{-5}$). The exciton transitions may be associated with the temperature-dependent structure seen by Iqbal, Christoe, and Dawson¹⁰ in the C \equiv N stretching region.

VI. ELECTRON-PHONON INTERACTION

An interesting feature of the data is the strength and polarization of the conductivity peaks in the molecular stretching region (1000–2000 cm^{-1}). These modes are, in the molecule, polarized in the molecular plane. In this salt, however, the modes are largely polarized along the chain axis which is nearly perpendicular to the molecular planes. Furthermore, these modes have an oscil-

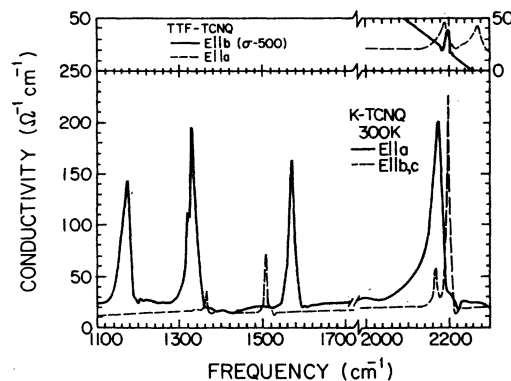


FIG. 6. Main graph: Real part of the conductivity of K-TCNQ between 1100 and 1700 cm^{-1} and between 2000–2300 cm^{-1} . Data are shown for both polarizations. Upper part: Real part of the conductivity of TTF-TCNQ between 2000 and 2300 cm^{-1} . For the electric field parallel to the conductivity axis, the data are plotted as $\sigma_1(\omega) - 500 \Omega^{-1} \text{cm}^{-1}$.

lator strength which is at least an order of magnitude larger than a molecular stretching mode oscillator strength. This effect has been noted by Anderson and Devlin⁷ in studies of K-TCNQ and has also been noted in charge-transfer salts of the radical salt tetracyanoethelene (TCNE).²³ Similar, but even larger effects have been observed in TEA-(TCNQ)₂ by Kaplunov, Panova, and Borodko²⁴ and by Brau *et al.*²⁵ In TEA-(TCNQ)₂ the molecular stretching modes are superimposed on a strong electronic absorption while in K-TCNQ the molecular and electronic absorptions are rather neatly separated in frequency. The conductivity in this region is shown in more detail in Fig. 6. The conductivity peaks for $\vec{E} \parallel \vec{a}$ are seen to be both higher and broader than for $\vec{E} \parallel \vec{b}, \vec{c}$.

Recently Rice, Duke, and Lipari²⁶ and Rice⁵ have been studying the electron-intramolecular coupling in TCNQ salts and have derived an expression for the conductivity which is very similar to the Lee, Rice, and Anderson²⁷ expression for the conductivity of the (pinned) Frohlich mode in one-dimensional conductors. If $\omega < 2\Delta$, where 2Δ is the electronic energy gap ($2\Delta \sim \omega_{sp}$ here), and if the phonon modes are well separated compared to their widths, the conductivity calculated by Rice⁵ may be cast into the following Lorentzian form:

$$\sigma_1(\omega) = \text{Re} \sum_n \frac{N_n^2}{M_n^*} \frac{\omega}{\omega \Gamma_n + i(\omega_n^2 - \omega^2)} + \sigma_{1sp}(\omega), \quad (3)$$

where σ_{1sp} is the contribution to the conductivity of excitons across the gap,

$$M_n^* = m^* [(2\Delta)^2 / \lambda_n \omega_n^2] [f(\omega/2\Delta)]^2 \quad (4)$$

is the effective mass,

$$\bar{\omega}_n = \omega_n \left[1 - \frac{\lambda_n}{\lambda} \left(1 - \frac{V}{\Delta} \right) - \lambda_n \left(\frac{\omega}{2\Delta} \right)^2 f \left(\frac{\omega}{2\Delta} \right) \right]^{1/2} \quad (5)$$

is the loaded frequency, ω_n is the bare frequency, Γ_n is the width, and λ_n is the dimensionless electron-phonon coupling constant of the n th phonon mode. The index n runs over all of the symmetry-allowed optically active phonon modes. Other parameters are N , the electron density (one per TCNQ molecule); m_b , the electron band mass; V , the crystal potential, and

$$f(X) = \frac{\tan^{-1}[X/(1-X^2)^{1/2}]}{X(1-X^2)^{1/2}} \xrightarrow{x \rightarrow 0} 1 + X^2. \quad (6)$$

The dimensionless electron-phonon coupling constant is $\lambda = \sum_n \lambda_n$. Within Rice's model the phonons to which the electrons are coupled are the A_g totally symmetric vibrational modes of the TCNQ molecule. Normally, these modes are infrared inactive and Raman active, but, due to their coupling to the electron gas, they become infrared active with polarization parallel to the direction of electronic polarizability.

The plausibility of the model can be seen by a simple physical argument. It is well known that bond lengths in the TCNQ molecule change when an electron is added to make the ion. These bond length changes are symmetric and correspond to static displacements in the normal coordinates of the A_g modes. If the crystal is polarized by an infrared electric field of frequency $\omega < 2\Delta$, the bond length will be modulated at this frequency. There will be peaks in the conductivity wherever the infrared frequency equals one of the mode frequencies. If the electronic energy gap is such that

$\omega > 2\Delta$ then the large amplitude of the phonon modes at resonance tends to scatter the carriers and reduce the current. The affect is to reduce the conductivity; the modes are seen as antiresonances.

The effective electron-phonon coupling constants for the data in Fig. 6 can be found from either Eq. (4) for the effective mass or Eq. (5) for the shifted frequency. We have chosen to work with the effective mass because we do not know V , the crystal potential, or the frequencies of the A_g modes in the TCNQ⁻ ion in the absence of electron-phonon coupling. Results for K-TCNQ are shown in Table I. The upper part is the data for $\vec{E} \parallel \vec{a}$, the lower for $\vec{E} \parallel \vec{b}, \vec{c}$. Column 1 gives the frequencies of the modes. The next two columns give the frequency and characterization of the stretching modes in neutral TCNQ as determined by Takenaka²⁸ and Girlando and Pecile.²⁹ The shifts are seen to be to lower frequencies in agreement with Eq. (5). The next two columns give the mass M (in units of 10^3 electron masses) found from integrating the absorption peak after subtracting out the background conductivity and making the following definition

$$\int_{\omega^-}^{\omega^+} \sigma_1^{pk}(\omega^1) d\omega^1 = \frac{\pi N e^2}{2M^*}, \quad (7)$$

where N is taken as one (electron) per TCNQ molecule. The limits of integration are from well below the mode to well above it. The last column gives the value for λ_n (for $\vec{E} \parallel \vec{a}$) calculated from Eq. (4) using the observed phonon frequency and $2\Delta = \omega_{sp} = 7520 \text{ cm}^{-1}$ (0.9 eV). We find $\lambda^{\text{opt}} = \sum \lambda_n \approx 0.10$ where λ^{opt} is the total electron-optical phonon cou-

TABLE I. Parameters of K-TCNQ molecular modes.

Frequency (cm ⁻¹)	Frequency in TCNQ ^o (cm ⁻¹)	Characterization	Mass 10 ³ M _b	Electron-phonon coupling constant
325	334	Ring deformation	~30	~0.02
477	602	C(CN) ₂ sissor	18	0.015
$\vec{E} \parallel \vec{a}$ 715	711	C-C stretch wing and ring	11	0.011
822	948	C-C ring stretch, C(CN) ₂ sissor	7.6	0.010
1174	1207	C-H bend, C=C ring stretch	2.6	0.014
1320 } 1330 }	1454	C=C wing stretch	12 } 2.3 } 2.0	0.015
1571	1602	C=C ring stretch C-H bend	3.2	0.006
2175	2229	C≡N stretch	1.3	0.008
1365	1405	C-H bend	50	
1508	1540	C=C ring stretch	18	
$\vec{E} \parallel \vec{b}, \vec{c}$ 2167 } 2198 }	2228	C≡N stretch	14 3.4	

pling constant. This value does not include the contribution from modes below 300 cm^{-1} . There is an A_g mode at 224 cm^{-1} in TCNQ^0 which, because $\lambda_n \sim 1/\omega_n^2$, could have a sizeable contribution. There could also be contributions from low-lying lattice modes.

Strictly speaking, this model should not apply to the half-filled band case (such as K-TCNQ) because the phase (infrared active) and amplitude (infrared inactive) collective modes become the same (inactive) mode. This seems to be a general feature of solving the Fröhlich Hamiltonian within a half-filled tight-binding model.³⁰ It is probably a mathematical artifact and would not occur within any real band structure. Clearly, the effects described above are seen in K-TCNQ.

Another interesting case is that of the highly conducting salt TTF-TCNQ. At the top of Fig. 6 is shown the conductivity of TTF-TCNQ in the $C \equiv N$ stretching region for both polarizations.¹⁹ The vertical scale is the same as in the main figure. For $\vec{E} \parallel \vec{a}$ there are two modes of nearly equal strength; the lower-frequency one at 2190 cm^{-1} is the $C \equiv N$ stretch, while the upper-frequency one at 2270 cm^{-1} is the $C-D$ stretch. The data for $\vec{E} \parallel \vec{b}$ is superimposed on an electronic background from the energy gap so we have plotted $\sigma(\omega) - 500\ \Omega^{-1}\text{ cm}^{-1}$. The coupling of the electrons to this $C \equiv N$ stretching mode in TTF-TCNQ is very weak. None of the other molecular stretching modes were definitely visible in our data, as peaks. Since the frequency is greater than the gap, however, the model predicts that these modes should be visible as antiresonances or dips in $\sigma_1(\omega)$. As has been pointed out previously,^{31,32} several dips in $\sigma_1(\omega)$ for TTF-TCNQ could be associated with electron-optical phonon coupling effects. The most obvious one extends from 1100 to 1800 cm^{-1} , and is actually two minima, at 1350 and 1450 cm^{-1} . For $\omega > 2\Delta$, $\sigma_1(\omega)$ can be found by substituting Eqs. (4) and (5) into Eq. (3) and using

$$f(X) = \left\{ \ln \left(\frac{1 - (1 - X^{-2})^{1/2}}{1 + (1 - X^{-2})^{1/2}} \right) + \pi i \right\} / 2X(1 - X^{-2})^{1/2}. \quad (8)$$

This function is now complex. The coupled-electron-phonon contribution to $\sigma_1(\omega)$ is negative. For $\omega \sim 2\Delta$, the results of this model are strongly dependent upon the numerical values of the gap. Using $2\Delta \approx 1100$ as determined from infrared studies,¹⁷ one can estimate $\lambda_n \approx 0.03$ for $\tilde{\omega}_n = 1350\text{ cm}^{-1}$ and $\lambda_n \approx 0.04$ for $\tilde{\omega}_n = 1450\text{ cm}^{-1}$.

In the light of the results presented above and those found in $\text{TEA}-(\text{TCNQ})_2$ it is clear that the TCNQ salts form an excellent system for the study of electron-phonon interactions in solids. The theory can be compared with experimental results in

three cases; all of the values for λ_n are about the same: $\lambda_n \sim 0.01-0.02$. There does not seem to be a big effect in the numbers obtained when the material is conducting or when the electronic absorption overlaps with the phonon frequencies.

VII. SUMMARY AND CONCLUSIONS

In this study we have measured the polarized reflectance of K-TCNQ and performed a Kramers-Kronig analysis of the data. From these data we make three main points.

(i) The electronic absorption for $\vec{E} \parallel \vec{a}$ (chain axis) is a maximum at 7520 cm^{-1} (0.9 eV) and has a broad asymmetric wing on the high-frequency side. From a fit to the conductivity we obtain values for the single-particle gap $\omega_{sp} = 0.9\text{ eV}$, and electron relaxation time $\tau = 2.6 \times 10^{-15}\text{ s}$. To obtain a good fit to the data we require two Lorentzian modes and we conclude that there is some evidence for at least two electronic absorptions in K-TCNQ for frequencies between 6000 and 15000 cm^{-1} . If this is the case, the entire interpretation of optical properties of TCNQ salts made by Torrance, Kaufman, and Scott¹ is not correct.

(ii) The oscillator strength for $\vec{E} \parallel \vec{a}$ is very small until the frequency becomes larger than 5000 cm^{-1} (0.6 eV) where it rises very rapidly. At frequencies corresponding to the activation energy calculated from magnetic resonance measurements,⁴ 2000 cm^{-1} (0.24 eV), only 1% of the interband oscillator strength is used up. This supports the conclusion of Khanna *et al.*² that this magnetic excitation is a spin-wave mode located in the single-particle gap.

(iii) The molecular stretching modes show effects of electron-optical phonon coupling. These lead to a series of collective modes at frequencies near the totally symmetric A_g phonon frequencies, polarized along the chain axis. We have calculated the electron-phonon coupling constants following the discussion of Rice.⁵ The value for $\lambda^{\text{opt}} \sim 0.1$.

Note added in proof. It was pointed out to us by Professor C. Pecile that the assignments of the 477-cm^{-1} and 822-cm^{-1} modes (Table I) may be incorrect; see Ref. 29 for details. Since this paper was submitted M. J. Rice, N. Lipari, and S. Strässler have constructed a theory appropriate to the dimerized half-filled band case which allows an unambiguous determination of the electron-molecular vibration coupling constants. They find $\lambda = \sum_{m=2}^9 \lambda m \approx 0.3$, somewhat larger than the estimates in Table I.

ACKNOWLEDGMENTS

We thank Dr. M. J. Rice for a preliminary version of his paper prior to publication and for sev-

eral helpful discussions on the effects of electron-phonon interaction on the intramolecular mode enhanced oscillator strengths. We thank Professor A. F. Garito for help with the materials and useful

discussions. The high-quality crystals which made this reflectance study possible were grown by Paul Nigrey.

*Present address: Physics, Lab III, Technical University of Denmark, DK-2800 Lyngby, Denmark.

†Present address: Union Carbide Research Center, Parma, Ohio.

[‡]Work at the University of Pennsylvania supported by the NSF through Grant No. DMR-74-22923 and through the University of Pennsylvania Materials Research Laboratory Grant No. (DMR-76-00678), and by the Advanced Research Projects Agency through Grant No. DAHC-15-72-C-0174.

¹J. B. Torrance, B. A. Scott, and F. B. Kaufman, *Solid State Commun.* **17**, 1369 (1975).

²S. K. Khanna, A. A. Bright, A. F. Garito, and A. J. Heeger, *Phys. Rev. B* **10**, 2139 (1974).

³Johan G. Vegter and Jan Kommandeur, *Phys. Rev. B* **9**, 5150 (1974).

⁴T. Hibma and J. Kommandeur, *Solid State Commun.* **17**, 259 (1975).

⁵M. J. Rice, *Phys. Rev. Lett.* **37**, 36 (1976).

⁶Shoji Hiroma, Haruo Kuroda, and Hideo Akamatu, *Bull. Chem. Soc. Jpn.* **44**, 9 (1971).

⁷George R. Anderson and J. Paul Devlin, *J. Phys. Chem.* **79**, 1100 (1975).

⁸Yoichi Iida, *J. Chem. Soc. Jpn.* **42**, 71 (1969).

⁹Y. Oohashi and T. Sakata, *Bull. Chem. Soc. Jpn.* **46**, 3330 (1973).

¹⁰Zafar Iqbal, C. W. Christoe, and D. K. Dawson, *J. Chem. Phys.* **63**, 4485 (1975).

¹¹Johan Vegter, Tjip Hibma, and Jan Kommandeur, *Chem. Phys. Lett.* **3**, 427 (1969).

¹²A. Hoehstra, T. Spoelda, and A. Vox, *Acta Crystallogr. B* **28**, 14 (1971).

¹³See, for example, F. Wooten, *Optical Properties of Solids* (Academic, New York, 1971), Appendix A.

¹⁴J. Murgich and S. Pissantzky, *Chem. Phys. Lett.* **18**, 420 (1973).

¹⁵F. Denoyer, R. Comes, A. F. Garito, and A. J. Heeger, *Phys. Rev. Lett.* **35**, 445 (1975).

¹⁶S. Kagoshima, H. Anzai, K. Kajimura, and T. Ishiguro, *J. Phys. Soc. Jpn.* **39**, 1143 (1975).

¹⁷R. Comes, S. M. Shapiro, G. Shirane, A. F. Garito, and A. J. Heeger, *Phys. Rev. Lett.* **35**, 1518 (1975).

¹⁸M. A. Butler, F. Wudl, and Z. G. Soos, *Phys. Rev. B* **12**, 4708 (1975).

¹⁹D. B. Tanner, C. S. Jacobsen, A. F. Garito, and A. J. Heeger, *Phys. Rev. B* **13**, (1976).

²⁰P. Breusch, S. Strassler, and H. R. Zeller, *Phys. Rev. B* **12**, 219 (1975).

²¹P. M. Grant, R. L. Greene, and G. Castro, *Bull. Am. Phys. Soc.* **20**, 496 (1975).

²²J. J. Ritsko, D. J. Sandman, A. J. Epstein, A. C. Gibbons, S. E. Schnatterly, and J. Fields, *Phys. Rev. Lett.* **34**, 1330 (1975).

²³See for example, Jerold J. Hinkel and J. Paul Devlin, *J. Chem. Phys.* **58**, 4750 (1973), and references therein.

²⁴M. G. Kapluna, R. P. Panova, and Y. G. Borodko, *Phys. Status Solidi A* **13**, K67 (1972).

²⁵A. Bray, P. Bruesch, J. P. Farges, W. Hinz, and D. Kuse, *Phys. Status Solidi B* **62**, 615 (1974).

²⁶M. J. Rice, C. B. Duke, and N. O. Lipari, *Solid State Commun.* **17**, 1089 (1975).

²⁷P. A. Lee, T. M. Rice, and P. W. Anderson, *Solid State Commun.* **14**, 703 (1974).

²⁸Tohru Takenaka, *Spectrochim. Acta A* **27**, 1725 (1971).

²⁹A. Girlando and C. Pecile, *Spectrochim. Acta* **29**, 1859 (1973).

³⁰See, for example, Bruce R. Patton and L. J. Sham, *Phys. Rev. Lett.* **31**, 631 (1973); **33**, 638 (1974).

³¹J. B. Torrance, E. E. Simonyec, and A. N. Bloch, *Bull. Am. Phys. Soc.* **20**, 273 (1975).

³²H. Gutfreund, B. Horowitz, and M. Weger, *Solid State Commun.* **15**, 849 (1974).